Simulating passivity for Robotic Walkers via Authority-Sharing

Marco Andreetto, Stefano Divan, Francesco Ferrari, Daniele Fontanelli, Luigi Palopoli and Fabiano Zenatti

***Abstract*—We consider a robotic walking assistant used to guide senior users across a crowded space. The problem we address is how to guide the user using motorised back wheels. Our strategy aims to simulate a passive behaviour in which the forward velocity is the one imposed by the user, who receives the impression of controlling the motion. The result is obtained leaving the user in control (without any actuation) when she/he follows straight lines, while the motors kick in when the user has to make a turn. We offer extensive theoretical proof of the validity of our strategy. The technique has been validated via extensive experimentation with a large group of older adults.**

***Index Terms*—Service Robots, Authority-Sharing.**

I. Introduction

THE ageing of the population of modern countries opens attractive research and market opportunities for robotics experts. In particular, service robots are becoming popular as intelligent mobility aids for older adults, while the reduced mobility of a large number of older adults is the recognised cause and the consequence of a number of physical problems and of the cognitive decline [1], [2]. The reason for the interest toward inexpensive and easy to use robotic mobility aids is motivated by their supposed efficacy in helping their users remain active beyond the walls of their houses.

An interesting example is given by the robotic walker *FriWalk*[3], whose main purpose is to act as a navigation aid and guide the user through the environment along a planned path that satisfies his/her requirements [4], [5]. The device is intended as a navigation aid rather than an autonomous assistive vehicle. For this reason, users should be guided without sacrificing their perceived freedom of movement. In this direction, very inspirational is the paradigm of passive robots [6], which leave the responsibility of the locomotion to the user. Straightforward ways to build a passive robot is either to use actuated steering wheels [7] or to resort to electromagnetic brakes for differential drive [8], [9]. In the latter case, optimal control minimising the braking torques have been recently presented [10]. To modulate the braking action, an appropriate sensing system is needed to estimate the torques applied by the user. In order to reduce the system final cost and its complexity, a bang-bang passive walker solution can be found in [11], in which the vehicle is turned on the left (right) blocking the left (right) rear wheel. The solution is simple (on/off control action) and inexpensive (no need of additional hardware for braking modulation). However, the small set of manoeuvres it produces enables a relatively accurate tracking of the path, although with a questionable user comfort [12]. To summarise, passive robotics is an interesting paradigm for assistive navigation systems, but it needs a combination of front steering wheels and brakes for safety reasons. Possible alternatives are the use complex and expensive hardwares (i.e., force sensors) or bang-bang strategies that diminish the user's comfort.

The use of an actuation for the back wheels of the vehicle will solve most of the problems, as the robot can generate a large set of "comfortable" manoeuvres. If needed an actuated walker can move autonomously and pick up a user in need in a remote location. Finally, the actuators can be used to generate emergency brakes for safety. Unfortunately, the presence of actuation disrupts the system passivity, with potential safety problems, which can be dealt with using direct or indirect user interfaces [13]. For the former, user commands/intentions are directly communicated to the device through joysticks [14], force sensors [15], [16], [17], turn buttons and voice commands/navigator support [18]. Indirect interfaces recognises user's movement and/or intent without requiring her/his input. For instance, the *JAIST* walker guesses the user's intention using laser scanned shin positions [19]; in [20] a depth camera is used to track the user limbs; in [21] current sensors and wheel rotational encoders are used to estimate the user applied forces.

The indirect interface adopted in this work preserves a safe and intuitive behaviour of the system without additional hardware, using *simulated passivity* with an actuated device following a desired path. A similar approach is in [22], where a motion control solution is applied to an omnidirectional robot equipped with force sensors. In our previous work [23], the passive behaviour is simulated by means of alternating phases when the user is in control and her/his forward speed is estimated, with phases in which the robot is in control and a slight braking steers it towards the desired path, if needed. As a result, the user receives the impression that he/she is moving at his/her desired pace as with a passive device (hence

Manuscript received: September, 10, 2017; Revised December, 6, 2017; Accepted January, 3, 2018.

This paper was recommended for publication by Editor John Wen upon evaluation of the Associate Editor and Reviewers' comments. This project has received funding from the European Unions Horizon 2020 Research and Innovation Programme - Societal Challenge 1 (DG CONNECT/H) under grant agreement n° 643644 "ACANTO - A CyberphysicAl social NeTwOrk using robot friends".

D. Fontanelli is with the Department of Industrial Engineering (DII), University of Trento, Via Sommarive 5, Trento, Italy daniele.fontanelli@unitn.it. M. Andreetto, S. Divan, F. Ferrari, L. Palopoli and F. Zenatti are with the Department of Information Engineering and Computer Science (DISI), University of Trento, Via Sommarive 5, Trento, Italy {marco.andreetto, stefano.divan, francesco.ferrari, luigi.palopoli, fabiano.zenatti}@unitn.it

Digital Object Identifier (DOI): see top of this page.

the name simulated passivity). The proposed paper extends the preliminary solution in [23] in four important directions. First, the vehicle controlled velocity is designed on the basis of the intensity of the correction and it is proportionate to the deviation, whereas in [23] a braking action was applied to the robot also to implement small corrections, thus reducing the comfort. This velocity adaptation still preserves the user safety guaranteeing that s/he is never pulled.

Second, the path following controller adopted here removes a singularity that was present in [23], thus ensuring global asymptotic stability, a better comfort and the safety. Third, the length of the two phase is adapted to the user behaviour, with a significant improvement on the system's performance. Finally, the system has been tested with a group of older adults and the quantitative and qualitative analysis of the results is reported in the paper. The users' evaluation gives a concrete grounding to our notion of comfort, which relates to the number of control actions and the adaptation to the user pace.

The paper is organised as follows. Section II presents the mathematical background, formalises the path following problem and gives an overview of the solution. Section III presents the details for the passivity simulation and the adopted control law, while Section IV describes how to combine the controller simulated passivity in an authority-sharing paradigm. The experimental results with the elderly are reported in Section V, while Section VI concludes the paper with some final remarks.

II. Problem formulation and Solution Overview

The vehicle is modelled as a unicycle like robot, having differential kinematics

$$[\dot{x}, \dot{y}, \dot{\theta}]^T = [v\cos\theta, v\sin\theta, \omega]^T, \tag{1}$$

where the coordinates $[x, y]$ define the position of the vehicle reference point, i.e. the mid point O_m of the rear axle, with respect to a fixed world frame $\langle W\rangle = \{O_w, X_w, Y_w, Z_w\}$ and θ is the orientation of the moving vehicle frame $\{O_m, X_m, Y_m, Z_m\}$ with respect to $\langle W\rangle$. The vehicle linear and angular velocities are denoted by v and ω, respectively. In this work, we explicitly make the assumption that $v > 0$, since it is reasonable to assume that the user usually pushes the rollator to move in the environment, while whenever the user imposes $v \leq 0$, he/she is performing on spot manoeuvres that do not require any control action. Under the hypothesis of pure wheel rolling motion, the vehicle velocities v and ω are linked to angular velocity of the rear wheels by

$$v = \frac{r(\omega_R + \omega_L)}{2}, \quad \omega = \frac{r(\omega_R - \omega_L)}{d}, \tag{2}$$

where ω_L and ω_R are the rotational velocities of the left and right wheel, respectively, r is the wheel radius and d is the length of the rear axle.

To properly represent the path following problem, we use a Frenet reference frame $\langle F\rangle = \{O_f, X_f, Y_f, Z_f\}$ moving along the path (see Figure 1). Let s be the curvilinear abscissa of the Frenet frame origin O_f, θ_d the desired yaw of the vehicle (i.e. the path orientation with respect to $\langle W\rangle$ in the point defined by s), and let $[l_x, l_y]$ be the coordinates of the vehicle reference point O_m in the Frenet frame. Define the

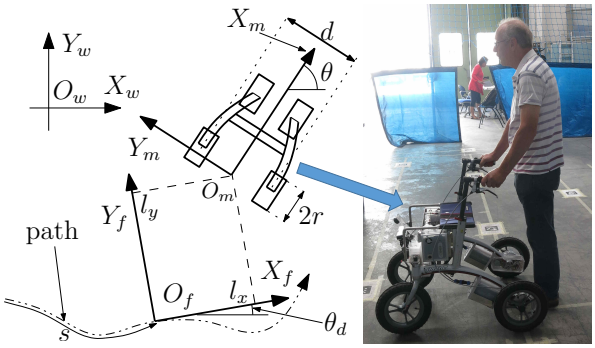

Figure 1. Adopted reference frames and coordinates.

vehicle orientation error as $\tilde{\theta} := \theta - \theta_d$. Using this new set of coordinates $[l_x, l_y, \tilde{\theta}]$, the differential kinematics of the vehicle (1) is rewritten as [24]

$$\begin{cases} \dot{l}_x &= -\dot{s}(1 - c(s)l_y) + v\cos\tilde{\theta}, \\ \dot{l}_y &= -c(s)\,\dot{s}\,l_x + v\sin\tilde{\theta}, \\ \dot{\tilde{\theta}} &= \omega - c(s)\dot{s}, \end{cases} \tag{3}$$

where $c(s) = \frac{\mathrm{d}\theta_d}{\mathrm{d}s}(s)$ is the path curvature and the velocity $\dot{s}$ of the Frenet frame is an auxiliary control input. The state of the vehicle can be equivalently represented as $\chi = [l_x, l_y, \tilde{\theta}]^T$ or $\bar{\chi} = [x, y, \theta]^T$.

Using the coordinates $[l_x, l_y, \tilde{\theta}]$, the path following problem is considered solved if

$$\lim_{t\to+\infty} |l_x(t)| \leq l_\infty, \lim_{t\to+\infty} |l_y(t)| \leq l_\infty, \lim_{t\to+\infty} |\tilde{\theta}(t)| \leq \tilde{\theta}_\infty, \tag{4}$$

where t denotes the time, and $l_\infty > 0$ and $\tilde{\theta}_\infty > 0$ are positive arbitrary tolerated errors.

A. Solution overview

The path following problem (4) has to be solved using the available actuators, i.e. the rear motors. The motors are controlled to impose the wheel velocities ω_R and ω_L to the right and to the left wheel, respectively. According to (2), whenever the wheel velocities ω_R and ω_L are chosen, the vehicle velocities v and ω are defined as well. While the vehicle angular velocity ω can be chosen to control the yaw θ to approach and follow the path, the forward velocity v must be chosen by the user. In fact, in assistive robotics, because of user balance issues, it is extremely important that the vehicle does not pull the assisted person (i.e., by moving at a forward velocity larger than the one of the user). A possible way to face this issue is the use of *passive* robots that by definition do not have the authority on the vehicle forward velocity v [11], [7], [12]. In this work, instead, the robot is *active*, hence the motor velocities in (2) are used as input, therefore, as in [23], we propose to *simulate* the passivity of the vehicle by sharing the control authority between the user and the robot by alternating the following two working modes as shown in Figure 2:

Robot in control: The control authority is given to the robot. The wheel velocities ω_R and ω_L are controlled and the forward

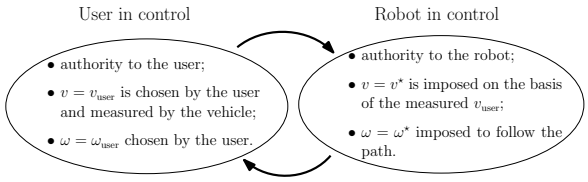

Figure 2. Simulation of passivity via authority-sharing.

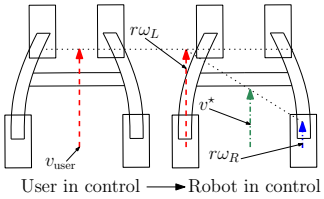

Figure 3. Computation of the vehicle velocities when the *Robot in control* mode is enabled and the vehicle has to turn right.

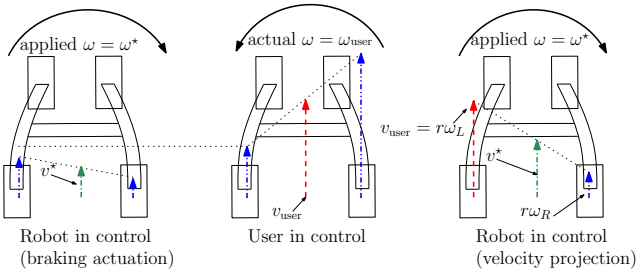

Figure 4. Difference between velocity projection and braking actuation for uncooperative users.

velocity $v = v^\star$ and the angular velocity $\omega = \omega^\star$ are imposed to the vehicle as in (2);

User in control: The control authority is given to the user. The motors are not activated, hence the vehicle is totally passive. Consequently, the vehicle velocities $v = v_{\text{user}}$ and $\omega = \omega_{\text{user}}$ are completely determined by the user and measured by the vehicle sensors, e.g. wheel encoders.

The passive behaviour in *Robot in control* mode is here simulated by imposing a controlled velocity $v^\star$ close (or even equal) to v_{user}, estimated in the *User in control* mode. This way, the user feels in control of the vehicle forward motion as if the robot were passive. As a consequence, to ensure that the path following requirements (4) are satisfied, in the *Robot in control* mode only the angular velocity $\omega^\star$ can be freely determined.

The overall controller implementing simulated passivity via authority-sharing is then composed by two ingredients: (i) a path following control law ensuring (4) and simulating a passive robot, i.e. suitably computing the forward velocity $v^\star$ given the desired user velocity v_{user}, to be applied in the *Robot in control* mode; (ii) a switching strategy between the two modes based on the user behaviour and implementing the simulated passivity via authority-sharing paradigm.

III. Simulating passivity in *Robot in control* mode

The path following problem (4) is decoupled in two subproblems. In order to simulate passivity and to improve the user balance, the robot should not pull the assisted person, that is the vehicle should not increase the speed v_{user}. To this end, we design two alternative strategies to compute $v^\star$, whose on-line selection is determined as described in Section III-A. Then, we design a control law $\omega = \omega^\star(\chi)$ that correctly steers the vehicle regardless of the forward velocity v of the vehicle.

A. Forward velocity selection to simulate passivity

1) Velocity projection: Whenever the angular velocity $\omega \neq 0$, one of the two wheels has a larger velocity than the vehicle reference point velocity v (according to Equation (2)). For instance, if the vehicle turns right, the left wheel is faster than both the right wheel and v. Therefore, since the walker handles are approximately located above the rear wheels and even if the applied controlled velocity $v^\star \leq v_{\text{user}}$, the user may feel to be pulled by the fastest wheel. Hence, we impose that the fastest point of the vehicle has a forward velocity equal to v_{user}. In particular, if the requested angular velocity is positive, i.e. $\omega^\star > 0$, the vehicle turns left and the right wheel, the fastest one, is set to $\omega_R = v_{\text{user}}/r$. According to (2), we finally get

$$v^\star = v_{\text{user}} - \omega^\star \frac{d}{2}, \quad \omega_L = \frac{v_{\text{user}}}{r} - \omega^\star \frac{d}{r}.$$

The case of $\omega^\star < 0$ is homologous. A compact formula to describe this strategy is $v^\star = v_{\text{user}} - |\omega^\star|\frac{d}{2}$. An example of the proposed algorithm is in Figure 3.

2) Braking actuation: Since the motors directly command the wheel velocities, projecting the user's velocity v_{user} on the fastest wheel might still generate discomfort if the correction that the robot has to apply is relevant. Consider for example Figure 4. In the *User in control* mode (centre of the figure) the user is steering the vehicle left. Suppose that, when the *Robot in control* mode is enabled, the vehicle has to turn right. If the velocity projection strategy is applied, the velocity of the left wheel may increment and still compromise the user's balance if the difference between angular the velocities is relevant (right part of Figure 4). To avoid such a condition, the vehicle is braked by setting $v^\star = \alpha v_{\text{user}}$, where $\alpha < 1$ in order to ensure a braking action and avoid that the user is pulled by the left handle (left part of Figure 4).

3) Choice of the forward velocity: The rationale of the forward velocity $v^\star$ choice in the *Robot in control* mode is the following. If the robot intervention considerably varies the vehicle angular velocity ω, the braking actuation method is applied to guarantee the user's safety. Conversely, if the robot can apply a small correction only (i.e. the required angular velocity $\omega^\star$ is close to the actual ω), the velocity projection method is applied to improve the user's comfort. Overall, the forward velocity simulating passivity applied in the *Robot in control* mode is

$$v^\star = \begin{cases} v_{\text{user}} - |\omega^\star|\dfrac{d}{2}, & \text{when } |\omega - \omega^\star| \leq \Omega, \\ \alpha v_{\text{user}}, & \text{when } |\omega - \omega^\star| > \Omega, \end{cases} \tag{5}$$

where $\Omega > 0$ and α are two comfort parameters to be tailored on the specific user's requirements.

B. Path Following Controller

It is a common practice in path following problems, to define an approaching angle function $\delta(\cdot)$ defining the manoeuvre that the vehicle has to take to approach and follow the path like in [24], [25]. In the rest of this section we will prove that if $\delta(\cdot)$ is a function of l_y in (3) and satisfies some mild assumptions, the path following problem (4) is solved with $l_\infty = \tilde{\theta}_\infty = 0$ if $e_\theta \triangleq \tilde{\theta} - \delta(l_y)$ converges to zero, where $\tilde{\theta}$ is again reported in (3). The auxiliary control input $\dot{s}$ is designed to stabilise the path following error l_x.

Theorem 1 (Attitude stabilisation): Consider the vehicle kinematic model (3) and assume that the vehicle in persistent motion, i.e. the forward velocity $v \geq 0$ satisfies $\lim_{t\to\infty} v(t) \neq 0$, and that the approaching angle $\delta(l_y)$ is differentiable, strictly monotonic and odd satisfying $l_y\delta(l_y) \leq 0$ and $|\delta(l_y)| \leq \frac{\pi}{2}\, \forall l_y$. Then the control law

$$\omega = \omega^\star(\chi) = v\left(\gamma(\chi) - \kappa\left(\tilde{\theta} - \delta(l_y)\right)\right), \tag{6}$$

where κ is a constant gain such that $v\kappa > 0$ and

$$\begin{aligned} \gamma(\chi) &= c(s)\dot{\xi} + \left(-c(s)\,\dot{\xi}\, l_x + \sin\tilde{\theta}\right)\frac{\mathrm{d}\delta}{\mathrm{d}l_y}(l_y), \\ \dot{s} &= v\dot{\xi}, \\ \dot{\xi} &= \cos(\tilde{\theta}) + \kappa_x l_x, \end{aligned} \tag{7}$$

with $\kappa_x > 0$, ensures that the attitude error $e_\theta = \tilde{\theta} - \delta(l_y)$ converges to zero.

Assumption 2: Consider the Lyapunov function $V = \frac{1}{2}e_\theta^2$, whose derivative along the solutions is

$$\dot{V} = e_\theta \dot{e}_\theta = e_\theta\left(\omega - c(s)\dot{s} - \dot{l}_y\frac{\mathrm{d}\delta}{\mathrm{d}l_y}(l_y)\right) = e_\theta\left(\omega - v\gamma(\chi)\right).$$

By imposing $\omega = \omega^\star(\chi)$ in (6), we get

$$\dot{V} = -v\kappa e_\theta^2 < 0 \quad \forall e_\theta \neq 0,$$

that ensures the global convergence of e_θ to zero.

IV. Simulated passivity via authority-sharing

The overall vehicle passive behaviour is simulated by sharing the control authority by switching between the *User in control* mode and the *Robot in control* mode, as depicted in Figure 2. The switching strategy is synthesised with a synergistic use of two different ideas: a time based and a behavioural based approaches. More precisely, in the *User in control* mode, the vehicle behaves passively and estimates the user's velocity v_{user} for a time window T_U. In the *Robot in control* mode, the motors impose the velocities $v = v^\star$ and $\omega = \omega^\star(\chi)$ for a maximum time window of T_R, unless the user autonomously and approximately follows the path, where the control authority is given back to the user. This complex switching strategy is formalised using hybrid system theory [26].

A. Behavioural authority sharing

When the *Robot in control* mode is active but the user is autonomously following the path, i.e. when the path following errors are limited, the control authority is given back to the user. This is implemented by designing an hysteresis mechanism to the control law $\omega = \omega^\star(\chi)$. The mathematical formulation uses the hybrid dynamics of a logic variable $q \in \{0, 1\}$. When the vehicle is far from the path, we set $q = 1$ and the motors are engaged with velocities described in Section III. When the robot is close to the path, we set $q = 0$ and the motors are disengaged, i.e. totally passive walker. The switch between the two modes is activated with hysteresis on the basis of the distance from the path measured as $|e_\theta|$. In fact, because of the monotonicity property of the approaching angle $\delta(\cdot)$, it is sufficient to limit the attitude error e_θ to ensure that the path following requirements (4) hold. The hybrid dynamics of q is defined as

$$\begin{cases} \dot{q} &= 0, & [e_\theta, q]^T \in \mathcal{C}, \\ q^+ &= 1 - q, & [e_\theta, q]^T \in \mathcal{D}, \end{cases} \tag{8}$$

where $[e_\theta, q]^T$ is the overall state of the hybrid system, $\mathcal{C} := \mathcal{C}_0 \cup \mathcal{C}_1$ and $\mathcal{D} := \mathcal{D}_0 \cup \mathcal{D}_1$ are the flow and the jump set respectively, where

$$\begin{aligned} \mathcal{C}_0 &= \{|e_\theta| \leq \theta_{q_2} \ \wedge \ q = 0\}, \mathcal{C}_1 = \{|e_\theta| \geq \theta_{q_1} \ \wedge \ q = 1\}, \\ \mathcal{D}_0 &= \{|e_\theta| \geq \theta_{q_2} \ \wedge \ q = 0\}, \mathcal{D}_1 = \{|e_\theta| \leq \theta_{q_1} \ \wedge \ q = 1\}, \end{aligned} \tag{9}$$

where $\theta_{q_2} > \theta_{q_1} > 0$ are the hysteresis thresholds. Recalling (5) and (6), the actual velocities of the vehicle are then

$$v = (1-q)\, v_{\text{user}} + q v^\star \ \text{ and } \ \omega = (1-q)\, \omega_{\text{user}} + q\omega^\star(\chi), \tag{10}$$

and ensure the solution of the path following problem (4), as stated by the following theorem.

Theorem 3 (Path following): Consider the vehicle kinematic model (3) and the hypotheses of Theorem 1. Then, given two arbitrary non-negative constants l_∞ and $\tilde{\theta}_\infty$, there exists an upper hysteresis threshold θ_{q_2} such that the controller (10) ensures that the path following requirements (4) hold.

Assumption 4: Consider precautionary that controller (10) is never active (i.e. $q = 0$) if $|e_\theta| \leq \theta_{q_2}$. Theorem 1, in combination with the hybrid map defined by (9), ensures that $|e_\theta|$ enters in finite time and remains inside the region $|e_\theta| \leq \theta_{q_2}$. Once in this region, consider the Lyapunov function $V_2 = \frac{1}{2}l_x^2 + \frac{1}{2}l_y^2$, whose time derivative along the solutions is

$$\dot{V}_2 = l_x\left(-\dot{s} + v\cos\tilde{\theta}\right) + l_y v \sin\tilde{\theta}.$$

By substituting $\dot{s}$ from (7), we get

$$\dot{V}_2 = v\left(-\kappa_x\, l_x^2 + l_y \sin\tilde{\theta}\right) \leq v\, l_y \sin\tilde{\theta}.$$

Condition $\dot{V}_2 < 0$ is satisfied if $l_y \sin\tilde{\theta} < 0$, i.e. if $l_y \neq 0$, $\tilde{\theta} \neq 0$ and $\tilde{\theta} l_y < 0$. Since $\delta(\cdot)$ is an odd function of l_y, $\tilde{\theta} l_y < 0 \iff \tilde{\theta}\delta(l_y) > 0$. A sufficient condition for $\tilde{\theta}\delta(l_y) > 0$ is

$$|e_\theta| = |\tilde{\theta} - \delta(l_y)| < |\delta(l_y)|. \tag{11}$$

Because of the monotonicity of $\delta(\cdot)$, $|l_y| > l_y^\circ = \delta^{-1}(\theta_{q_2})$ implies $|\delta(l_y)| > \theta_{q_2}$. Therefore, inside region $|e_\theta| \leq \theta_{q_2}$, Equation (11) holds $\forall |l_y| > l_y^\circ$. Then

$$\dot{V}_2 < 0 \quad \forall |l_y| > l_y^\circ, \tilde{\theta} \neq 0. \tag{12}$$

Condition (12) ensures that $|l_y|$ enters in finite time and remains inside the region $|l_y| \leq l_y^\circ$. Inside this region, the monotonicity of $\delta(\cdot)$ implies that $|\delta(l_y)|$ is limited to $|\delta(l_y^\circ)| = \theta_{q_2}$. This bound on $\delta(l_y)$ inside the region $|e_\theta| = |\tilde{\theta} - \delta(l_y)| \leq \theta_{q_2}$, implies $|\tilde{\theta}| \leq \tilde{\theta}_\circ = 2\theta_{q_2}$ (indeed, $\tilde{\theta}_\circ$ is the analytic solution of the inequality $|\tilde{\theta} - \delta(l_y)| \leq \theta_{q_2}$ solved with respect to $\tilde{\theta}$ in the worst case $|\delta(l_y)| = |\delta(l_y^\circ)| = \theta_{q_2}$). Furthermore, once the solution enters the region $|l_y| \leq l_y^\circ$, we have $\dot{V}_2 = v\left(-\kappa_x\, l_x^2 + l_y \sin\tilde{\theta}\right) \leq v\left(-\kappa_x\, l_x^2 + l_y^\circ\right) \leq 0$, i.e.

$$\dot{V}_2 < 0, \quad \forall l_x > \sqrt{\frac{l_y^\circ}{\kappa_x}} = \sqrt{\frac{|\delta^{-1}(\theta_{q_2})|}{\kappa_x}} = l_x^\circ,$$

which implies that the solution enters in finite time and remains inside the region $|l_x| \leq l_x^\circ$. The proof follows by noticing that $\lim_{\theta_{q_2}\to 0} l_x^\circ = \lim_{\theta_{q_2}\to 0} l_y^\circ = \lim_{\theta_{q_2}\to 0} \tilde{\theta}^\circ = 0$, hence, given the tolerated errors l_∞ and $\tilde{\theta}_\infty$, one can always find an upper hysteresis threshold θ_{q_2} such that the path following conditions (4) hold.

Remark 1 (Nonsingular controller): In our previous work [23] a singularity was generated by the position of the Frenet on the point of the path closest to the vehicle. Intuitively, this happens when the vehicle is on the centre of the path curvature since the closest point on the path is not well defined. Inspired by [24], we have added a dynamic to the Frenet frame, which is modelled with $\dot{s}$ in (7). As consequence, the control law (6) is nonsingular and globally convergent at the price of three coordinates to express the path following, i.e. l_x, l_y and $\tilde{\theta}$ in (3), instead of just two as in [23]. This improvement is not only technical, but it is extremely beneficial and safer for the particular class of end-users of the system: indeed, close to the singularity of [23], the commanded angular velocity may be very large, hence yielding a sudden motion of the vehicle that may potentially harm the user's equilibrium.

B. Time based authority sharing

We introduce an additional logic variable p to describe the *Robot in control* mode. When $p = 0$, the *User in control* mode is active, while when $p = 1$ the *Robot in control* mode *can be* activated on the basis of the user behaviour logic variable q, described previously. Roughly speaking, p determines if the authority *can* be given to the robot, while q determines if the authority *is* given to the robot.

To model the activation time of the two control modes, we introduce two additional hybrid states τ_U and τ_R acting as timers. The timer of the *User in control* mode has hybrid dynamics

$$\begin{cases} \dot{\tau}_U &= 1 - p, & \tau_U \leq T_U, \\ \dot{p} &= 0, & p \in \{0,1\}, \\ \dot{h} &= 0, & h \in \{0,1\}, \end{cases} \tag{13}$$

$$\begin{cases} \tau_U^+ &= 0, & \tau_U = T_U, \\ p^+ &= \min(q, 1-p), & p \in \{0,1\}, \\ h^+ &= \max\left(\mathrm{sing}\left(\Omega - |\omega - \omega^\star|\right), 0\right), & h \in \{0,1\}, \end{cases} \tag{14}$$

where the logic variable $h \in \{0,1\}$ determines how the forward velocity should be computed, according to (5), i.e.

$$v^\star = h\left(v_{\text{user}} - |\omega^\star|\frac{d}{2}\right) + (1-h)\alpha v_{\text{user}}. \tag{15}$$

The discrete dynamics $p^+ = \min(q, 1-p)$ in (14) ensures that the *Robot in control* mode (i.e. the jump of p to 1) is activated when $\tau_U = T_U$ only if the user is not following the path, i.e. $q = 1$. The timer of the *Robot in control* mode has hybrid dynamics

$$\begin{cases} \dot{\tau}_R &= p, & \tau_R \leq T_R, \\ \dot{p} &= 0, & p \in \{0,1\}. \end{cases} \tag{16}$$

$$\begin{cases} \tau_R^+ &= 0, & \tau_R = T_R, \\ p^+ &= 1 - p, & p \in \{0,1\}. \end{cases} \tag{17}$$

Notice that, when $p = 1$, the continuous dynamics in (16) is design to increment the timer τ_R up to $\tau_R = T_R$. Then τ_R is reset to zero by the discrete dynamics in (17) and p jumps to 0 activating the dynamics (13) and (14). Finally, to ensure that the *User in control* mode immediately restarts when q jumps from 1 to 0, the discrete dynamics (8) is modified as

$$\begin{cases} \dot{q} &= 0, & [e_\theta, q]^T \in \mathcal{C}, \\ \dot{\tau}_R &= p, & [\tau_R, p]^T \in \mathbb{R}^2. \\ \dot{p} &= 0, \end{cases} \tag{18}$$

$$\begin{cases} q^+ &= 1 - q, & [e_\theta, q]^T \in \mathcal{D}, \\ \tau_R^+ &= (1-q)\tau_R, & [\tau_R, p]^T \in \mathbb{R}^2. \\ p^+ &= (1-q)p, \end{cases} \tag{19}$$

The result of the hybrid controller described in (13), (14), (16), (17), (18) and (19) is succinctly

$$v = \begin{cases} v_{\text{user}} & q = 0 \vee p = 0, \\ v^\star & \text{otherwise}, \end{cases}, \omega = \begin{cases} \omega_{\text{user}} & q = 0 \vee p = 0, \\ \omega^\star & \text{otherwise}. \end{cases}$$

C. Activation time tuning

The lengths of the activation times T_R and T_U clearly influence the user comfort and the path following performance and, hence, can be used as tuning parameters. Nevertheless, the effective values of these parameters are constrained. Indeed, the larger T_R, the better are the path following performance (authority is shifted to the robot). However, since in the *Robot in control* mode the user can not modify the vehicle velocities, T_R is precautionary upper bounded by a constant $T_R^{\max} > 0$. Conversely, the larger T_U, the larger is the user comfort. However, the path following error is larger with uncooperative users. As a consequence, to ensure that the path following requirements (4) hold even with an uncooperative user, the *User in control* mode should last for a small amount of time. According to Theorem 3, the performance is guaranteed as long as $|e_\theta| < \theta_{q_2}$ remains valid. The perturbation induced by the user can be quantified as

$$|\dot{e}_\theta^{\text{user}}| \leq |\omega_{\text{user}}| + |v_{\text{user}}\gamma(\chi)|,$$

hence the maximum increment of attitude error that the user can generate is $\Delta e_\theta = \int_{t_0}^{t_0+T_U} |\dot{e}_\theta^{\text{user}}| \mathrm{d}\tau$, where t_0 is the

time instant in which the *Robot in control* mode is activated. Clearly, if the user velocities are large, the time window T_U has to be small to limit Δe_θ. Therefore, an adaptive discrete dynamics is added to (17) and (19) (i.e. at the end of each *User in control* mode), reported next

$$T_U^+ = \min\left(\frac{a_1}{a_2|\hat{v}| + a_3|\hat{\omega}|}, T_U^{\max}\right), \quad T_U \in \mathbb{R}. \tag{20}$$

$\hat{v}$ and $\hat{\omega}$ are the measured vehicle velocities while a_1, a_2, and a_3 are constant parameters to be tuned on the specific user. $T_U^{\max} > 0$ is the upper bound to T_U in the *User in control* mode. The implementation of this $\min(\cdot)$ function is needed to avoid the undesired condition $T_U \to \infty$ whenever the vehicle is still (i.e. $\hat{v} = \hat{\omega} = 0$). Notice that these parameters could be set automatically in an adaptive tuning algorithm or by a GUI-based question & answers with the user. In both cases, the system should be used for a longer time than the one available for the field tests reported in Section V. Therefore, those parameters have been set via experiments with young testers (omitted for brevity) to guarantee an average behaviour between aggressive and loose control.

V. Experiments

In this section we present the experimental results of the proposed approach. Two studies were conducted in which the older adult participants completed different paths using the *FriWalk* in one laboratory of the University of Trento. In the first study (with 4 males, 10 females, ageing between 65 and 75 years old), the participants were asked just to travel along a couple of paths, while in the second study (with 6 males, 9 females, ageing between 64 and 100 years old) a more extensive study, with more than eight paths for each participants were considered. Some of the participants usually use walking aids, such as crutches and/or a walker (28.6% of *Study 1* and 43.8% of *Study 2*). Participants were contacted through the Municipality of Pergine Valsugana and the senior centre "Sempreverde" of Mattarello (both in the Trento province) and invited to participate. They were informed that data collection and that all information provided are covered by the ethical rules conceived for the ACANTO project [3] and that they could quit the experiment at anytime. Once consent was obtained they were invited to perform the tasks with the *FriWalk*. Before starting, an experimenter showed to the participant the path to follow and explained the features of the robotic walker and its motion modality. All participants completed a first trial (which was common for everybody) to take confidence with the robot walker and its movements. More than ten different paths, starting and ending in the same home position, were randomly chosen for each participant, that completed at least one of them. In the laboratory arena, three tables were placed to emulate an actual indoor environment (see the rectangular obstacles in Figure 5).

A. Quantitative analysis

We first present the quantitative analysis of the experimental results. The controller parameters adopted in the experiments are: $\alpha = 0.37$ and $\Omega = 0.08$ [rad/s] for (5), the hysteresis

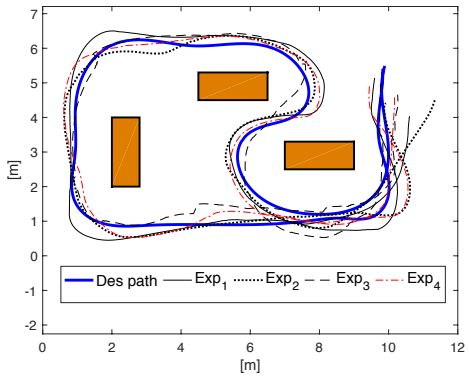

Figure 5. Experimental trajectories for four participants along a randomly selected path (solid thick line). The rectangles represent the obstacles (i.e. tables) in the environment.

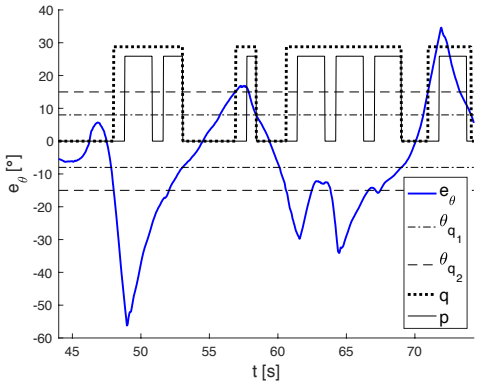

Figure 6. Last 30 seconds of the time evolution of the error e_θ for the Exp_1 in Figure 5. The evolution of the discrete hybrid variable p and q (scaled for visibility) and the controller thresholds θ_{q_1} and θ_{q_2} are also reported.

thresholds are set to $\theta_{q_1} = 8°$ and $\theta_{q_2} = 15°$, the maximum time for the *Robot in control* mode is $T_R = 2$ [s], while the parameters for the *User in control* mode in (20) are $T_U^{max} = 4$ [s], $a_1 = 2$, $a_2 = 2$ and $a_3 = 1$. Finally, we select $\delta(l_y) = -\pi/2 \tanh(l_y)$. Four sample trajectories along a randomly selected path are reported in Figure 5. The localisation is provided with an EKF [27] fusing the encoder data and the QR codes, positioned on the floor using the deployment [28] and read by the available front camera pointing downwards. It may happens that a QR code reading is missed, hence a localisation jump can be detected in the estimated trajectory (see the dashed trajectory of Exp_3 in Figure 5). Nonetheless, the controller is able to correctly steer the user towards the desired path. Figure 6 and Figure 7 reports the time evolution of the error e_θ and of the right ω_R angular velocity, respectively, for the last 30 seconds of the Exp_1 in Figure 5. It is important to recall that the user is in control when at least one of the two variables q or p is 0, which may happens, but for a limited amount of time (almost 0.8 seconds in the experiments) even if the robot is outside the hysteresis thresholds (see the portion of Figure 6 where $q \neq 0$ and $p = 0$). This is the essence of the time based authority sharing presented in Section IV-B, whereas

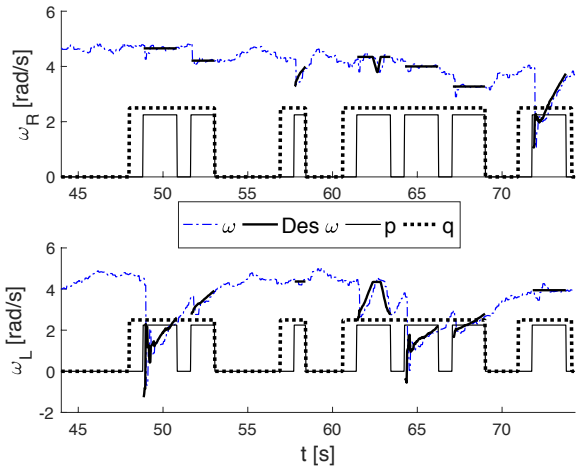

Figure 7. Last 30 seconds of the time evolution of the right ω_R (upper plot) and left ω_L (lower plot) angular velocities for the *Exp*$_1$ in Figure 5. The evolution of the discrete hybrid variable p and q (scaled for visibility) is also reported.

the behavioural authority sharing (Section IV-A) takes place whenever $q = p = 0$. Finally, it has to be noted how the controller is very effective in controlling the error e_θ in the region of the hysteresis (Figure 6).

For the actuation, it is evident from Figure 7 when the actuation kicks in by means of the desired velocity (thick solid lines superimposed to the actual wheels velocity, represented with a dash-dotted line). It is also noticeable how the wheel dynamic and the user applied forces generate a small tracking error of the desired velocity.

B. User's evaluation

In both studies, we used a questionnaire to conduct a structured interview to collect the impressions and opinions of people who participated in the studies. After the session with the robotic walker, participants were invited to sit next to an experimenter who conducted the structured interview reading the items of the questionnaire. The aim of the structured interview was to collect the impressions of people on the proposed control approach. To this end, we included different questions (open ended and closed ended). In the present work, we present the analysis of closed ended questions. Participants were asked to answer using yes or no and/or a 5 point Likert scale (1 "not at all", 2 "a little bit", 3 "moderately", 4 "very much", 5 "extremely"). The questions concerned different features of the interaction with the robotic walker, followed by items on the pleasantness of usage, the ease of learning, the control over the robot and its adaptability. Items used for the structured interview are shown in Table I. We first report the results of the characteristics of interaction in Table II. The percentage of affirmative responses, with their relative mean **M** and standard deviations **SD** on how much annoying/disturbing were the different features of the interaction on the Likert scale, are reported.

For the other items, the results, with mean and standard deviation, are summarised in Table III.

Table I
ITEMS OF THE QUESTIONNAIRE FOR THE USERS' EVALUATION.

Characteristics of the interaction
Vibration: Have you felt vibrations?
Path: Was it evident that was the walker to decide the path to follow?
Blocked: Have you felt to be pulled, pushed, pulled, or stuck?
If yes, How much unpleasant/annoying? was each feature.
Pleasantness (in using the *FriWalk*) - P
P.1: The experience with the walker was pleasant.
P.2: It was frustrating to carry out the task with the walker. *
P.3: You are satisfied with how he did the job with the walker.
Ease of learning - L
L.1: It was easy to learn to use the walker.
L.2: You could use the walker properly in a short time.
L.3: You had trouble understanding how to move around. *
Control over the *FriWalk* - C
C.1: You were sure the walker would always respond.
C.2: You had the impression you could suddenly miss the control. *
C.3: You had the impression you did not have full control. *
Adaptability of the walker - A
A.1: The walker fits well with your movements.
A.2: You had to adjust to the movements decided by the walker. *
A.3: The walker hindered/prevented your usual way of walking. *
* = Reversed

Table II
ANSWERS ON THE CHARACTERISTICS OF THE INTERACTION.

	Study 1		*Study 2*	
Item	**Yes**	**M (SD)**	**Yes**	**M (SD)**
Vibration	33.3%	1.75 (0.50)	53.3%	2.00 (0.76)
Path	91.7%	1.82 (0.98)	93.3%	1.31 (0.63)
Blocked	25%	2.00 (0.00)	66.7%	1.80 (0.79)

Discussion The results of the studies showed an overall positive impression of the *FriWalk*. Concerning the characteristics of interaction that in both studies most of the participants were aware that the *FriWalk* decided the path to follow, whereas a low percentage of them reported they felt the vibration and had the sensation of being blocked or pushed. In any case, we observed that participants did not perceive these features as disturbing or annoying, thus validating our definition of comfort. The results also showed that participants evaluated the experience as moderately pleasant and that they felt happy with their performance with the robot. Moreover, they reported they did not feel frustrated by the interaction with the walker. Importantly, from a user experience point of view, the participants reported they had the feeling they could always easily control the *FriWalk*. Finally, we found that participants had the feeling that the *FriWalk* well adapted to their speed and natural pace, so that the walker was not an obstacle to their usual way of walking.

Furthermore, it has been noted that participants showed good confidence in interpreting the walker suggestions with low path following errors. The fact that the *FriWalk* corrected the users by slightly slowing down was considered fundamental in this respect. Notice that in a few minutes participants understood the functioning of the robot and that with a clear explanation of its features and capabilities they did feel they were in control of the system.

Table III
MEANS AND STANDARD DEVIATION (IN PARENTHESIS) FOR THE QUESTIONNAIRE DESCRIBED IN TABLE I.

Study 1			
P - M (SD)	**L - M (SD)**	**C - M (SD)**	**A - M (SD)**
P1: 3.58 (0.79)	L1: 3.75 (0.45)	C1: 2.83 (1.34)	A1: 3.33 (1.07)
P2: 4.83 (0.58)	L2: 3.67 (0.49)	C2: 4.67 (0.89)	A2: 3.42 (1.24)
P3: 3.83 (0.72)	L3: 4.83 (0.39)	C3: 3.67 (1.23)	A3: 4.33 (0.89)
Study 2			
P - M (SD)	**L - M (SD)**	**C - M (SD)**	**A - M (SD)**
P1: 3.13 (0.74)	L1: 3.80 (0.68)	C1: 3.13 (0.92)	A1: 3.13 (0.74)
P2: 4.80 (0.56)	L2: 3.80 (0.56)	C2: 4.33 (0.82)	A2: 3.36 (0.74)
P3: 3.47 (0.74)	L3: 4.87 (0.35)	C3: 4.23 (0.93)	A3: 4.33 (0.82)

VI. CONCLUSIONS

In this paper, we have introduced a novel guidance solution for robotic walkers. The solution is based on alternating intervals in which the system is not engaged and the user is in control with other intervals in which the system comes into play to execute turns. The impression is that of a passive system in which the user is never "pulled" even if the turns are imposed using the motorised back wheels. We offer ample theoretical analysis revealing the asymptotic stability of the solution and its correct behaviour in presence of singularities. The system has been validated with a large base of senior users. We report both quantitative analysis and users evaluation of the *FriWalk*. From a technical perspective, future works will concentrate in changing dynamically the thresholds $\theta_{q_2} > \theta_{q_1} > 0$ according to the actual free space in front of the robot and still preserving the convergence properties. Moreover, future studies will focus on comparing different mechanical solutions and longer interactions with the robot walker using an ecological approach, and the possibility of orchestrating them with a visual feedback. Furthermore, learning algorithms to improve the user experience (i.e. tunable parameters or forward velocity adaptation) will be developed and tested.

REFERENCES

[1] L. Hedley, N. Suckley, L. Robinson, and P. Dawson, "Staying steady: a community-based exercise initiative for falls prevention," *Physiotherapy theory and practice*, vol. 26, no. 7, pp. 425–438, 2010.

[2] K.-T. Khaw, N. Wareham, S. Bingham, A. Welch, R. Luben, N. Day, *et al.*, "Combined impact of health behaviours and mortality in men and women: the epic-norfolk prospective population study," *Obstetrical and Gynecological Survey*, vol. 63, no. 6, pp. 376–377, 2008.

[3] "ACANTO: A CyberphysicAl social NeTwOrk using robot friends," http://www.ict-acanto.eu/acanto, February 2015, EU Project.

[4] A. Colombo, D. Fontanelli, A. Legay, L. Palopoli, and S. Sedwards, "Efficient customisable dynamic motion planning for assistive robots in complex human environments," *Journal of Ambient Intelligence and Smart Environments*, vol. 7, no. 5, pp. 617–633, 2015.

[5] L. Palopoli, A. Argyros, J. Birchbauer, A. Colombo, D. Fontanelli, *et al.*, "Navigation Assistance and Guidance of Older Adults across Complex Public Spaces: the DALi Approach," *Intelligent Service Robotics*, vol. 8, no. 2, pp. 77–92, 2015.

[6] A. Goswami, M. Peshkin, and J. Colgate, "Passive robotics: An exploration of mechanical computation," in *Proceedings of the 1990 American Control Conference*, 1990, pp. 2791–2796.

[7] M. Andreetto, S. Divan, D. Fontanelli, and L. Palopoli, "Harnessing Steering Singularities in Passive Path Following for Robotic Walkers," in *Proc. IEEE International Conference on Robotics and Automation (ICRA)*. Singapore: IEEE, May 2017, pp. 2426–2432.

[8] Y. Hirata, A. Hara, and K. Kosuge, "Motion control of passive intelligent walker using servo brakes," *IEEE Transactions on Robotics*, vol. 23, no. 5, pp. 981–990, 2007.

[9] Y.-H. Hsieh, K.-Y. Young, and C.-H. Ko, "Effective maneuver for passive robot walking helper based on user intention," *IEEE Transactions on Industrial Electronics*, vol. 62, no. 10, pp. 6404–6416, Oct 2015.

[10] D. Fontanelli, A. Giannitrapani, L. Palopoli, and D. Prattichizzo, "A Passive Guidance System for a Robotic Walking Assistant using Brakes," in *Proc. IEEE Int. Conf. on Decision and Control (CDC)*. Osaka, Japan: IEEE, 15-18 Dec. 2015, pp. 829–834.

[11] M. Andreetto, S. Divan, D. Fontanelli, and L. Palopoli, "Passive Robotic Walker Path Following with Bang-Bang Hybrid Control Paradigm," in *Proc. IEEE/RSJ International Conference on Intelligent Robots and System*. Daejeon, South Korea: IEEE/RSJ, Oct. 2016, pp. 1054–1060.

[12] ——, "Path Following with Authority Sharing between Humans and Passive Robotic Walkers Equipped with Low-Cost Actuators," *IEEE Robotics and Automation Letters*, vol. 2, no. 4, pp. 2271–2278, Oct. 2017.

[13] M. M. Martins, C. P. Santos, A. Frizera-Neto, and R. Ceres, "Assistive mobility devices focusing on smart walkers: Classification and review," *Robotics and Autonomous Systems*, vol. 60, no. 4, pp. 548 – 562, 2012.

[14] M. Martins, C. Santos, A. Frizera, and R. Ceres, "Real time control of the asbgo walker through a physical human-robot interface," *Measurement*, vol. 48, no. Supplement C, pp. 77 – 86, 2014.

[15] B. Graf, "An adaptive guidance system for robotic walking aids," *CIT. Journal of Computing and Information Technology*, vol. 17, no. 1, pp. 109–120, 2009.

[16] C.-K. Lu, Y.-C. Huang, and C.-J. Lee, "Adaptive guidance system design for the assistive robotic walker," *Neurocomputing*, vol. 170, no. Supplement C, pp. 152 – 160, 2015.

[17] Y. Wang and S. Wang, "A new directional-intent recognition method for walking training using an omnidirectional robot," *Journal of Intelligent & Robotic Systems*, vol. 87, no. 2, pp. 231–246, Aug 2017.

[18] V. Kulyukin, A. Kutiyanawala, E. LoPresti, J. Matthews, and R. Simpson, "iwalker: Toward a rollator-mounted wayfinding system for the elderly," in *2008 IEEE International Conference on RFID*, April 2008, pp. 303–311.

[19] G. Lee, T. Ohnuma, and N. Y. Chong, "Design and control of jaist active robotic walker," *Intelligent Service Robotics*, vol. 3, no. 3, pp. 125–135, Jul 2010.

[20] S. Taghvaei, Y. Hirata, and K. Kosuge, "Control of a passive walker using a depth sensor for user state estimation," in *2011 IEEE International Conference on Robotics and Biomimetics*, Dec 2011, pp. 1639–1645.

[21] S. Y. Jiang, C. Y. Lin, K. T. Huang, and K. T. Song, "Shared control design of a walking-assistant robot," *IEEE Transactions on Control Systems Technology*, vol. 25, no. 6, pp. 2143–2150, Nov 2017.

[22] O. Y. Chuy, Y. Hirata, Z. Wang, and K. Kosuge, "A control approach based on passive behavior to enhance user interaction," *IEEE Transactions on Robotics*, vol. 23, no. 5, pp. 899–908, Oct 2007.

[23] M. Andreetto, S. Divan, D. Fontanelli, L. Palopoli, and F. Zenatti, "Path Following for Robotic Rollators via Simulated Passivity," in *Proc. IEEE/RSJ International Conference on Intelligent Robots and System (IROS)*. Vancouver, Canda: IEEE/RSJ, Oct. 2017, to appear.

[24] D. Soetanto, L. Lapierre, and A. Pascoal, "Adaptive, non-singular path-following control of dynamic wheeled robots," in *IEEE Conf. on Decision and Control*, vol. 2. IEEE, 2003, pp. 1765–1770.

[25] A. Wachaja, P. Agarwal, M. Zink, M. R. Adame, K. Mller, and W. Burgard, "Navigating blind people with a smart walker," in *2015 IEEE/RSJ International Conference on Intelligent Robots and Systems (IROS)*, Sept 2015, pp. 6014–6019.

[26] R. Goebel, R. G. Sanfelice, and A. R. Teel, *Hybrid Dynamical Systems: modeling, stability, and robustness*. Princeton University Press, 2012.

[27] P. Nazemzadeh, F. Moro, D. Fontanelli, D. Macii, and L. Palopoli, "Indoor Positioning of a Robotic Walking Assistant for Large Public Environments," *IEEE Trans. on Instrumentation and Measurement*, vol. 64, no. 11, pp. 2965–2976, Nov 2015.

[28] P. Nazemzadeh, D. Fontanelli, and D. Macii, "Optimal Placement of Landmarks for Indoor Localization using Sensors with a Limited Range," in *International Conference on Indoor Positioning and Indoor Navigation (IPIN)*. Madrid, Spain: IEEE, Oct. 2016, pp. 1–8.